International Journal of Power Electronics and Drive System (IJPEDS)
Vol. 8, No. 2, June 2017, pp. 667~676
ISSN: 2088-8694, DOI: 10.11591/ijpeds.v8i2.pp667-676

Shunt Active Filter Based on Radial Basis Function Neural Network and p-q Power Theory

Prakash Ch.Tah[1], Anup K.Panda[2], Bibhu P.Panigrahi[3]
[1]Captive power Plant, SAIL Rourkela
[2]Department of Electrical Engineering, NIT Rourkela
[3]Department of Electrical Engineering, IGIT, Sarang

Article Info

Article history:

Received Jan 12, 2017
Revised Mar 12, 2017
Accepted Mar 27, 2017

Keyword:

Harmonics compensation
PI controller
p-q control strategy
RBFNN controller
Shunt active power filter
(SAPF)

ABSTRACT

In this paper a new combination of Radial Basis Function Neural Network and p-q Power Theory (RBFNN-PQ) proposed to control shunt active power filters (SAPF). The recommended system has better specifications in comparison with other control methods. In the proposed combination an RBF neural network is employed to extract compensation reference current when supply voltages are distorted and/or unbalance sinusoidal. In order to make the employed model much simpler and tighter an adaptive algorithm for RBF network is proposed. The proposed RBFNN filtering algorithm is based on efficient training methods called hybrid learning method. The method requires a small size network, very robust, and the proposed algorithms are very effective. Extensive simulations are carried out with PI as well as RBFNN controller for p-q control strategies by considering different voltage conditions and adequate results were presented.

Corresponding Author:

Anup K. Panda,
Department of Electrical Engineering, NIT Rourkela,
National Institute of Technology, India.
Email: akpanda.ee@gmail.com

1. INTRODUCTION

Recently following the deregulation and privatization of power industry the issue of power quality has been considered more and more by both the manufacturer and consumer of electricity. Modern electrical equipments including computers, rectifiers, inverters, ac regulator, vvf drives and other non linear loads are sensitive requiring higher power quality. On the other hand, these equipments are the origin of the same power quality phenomenon such as harmonics.Harmonics in power networks are one of the common problems related to power quality.

The most common power filters used to compensate harmonic voltages and currents are passive filters. Passive filters are cheap and easy to use, but they have low bandwidth (need several filters to compensate for a wide spectrum harmonic), can be subjected to resonance (series or parallel resonance with power system reactance), have large size (big capacitor banks or bulky inductors), and are affected by the source impedance [1]. However, active power filters (APF) have been introduced to overcome some of the problems of passive filters. An APF is dynamic, measure system parameters (current or/and voltage), calculates the reference signal, and injects a signal that meets the compensation objectives. In the compensation process, the APF decomposes a distorted signal into its fundamental, other harmonic components, reactive power, and other distortions (such as unbalanced waveforms). Several control strategies have been introduced to extract the reference current [2]-[6]. In recent times artificial intelligence techniques have been used for the generation of reference currents [7]-[15]. In general, there are two main methods for estimating harmonics; (i) parametric (such as artificial intelligence methods) and (ii) non-parametric (such as

fast Fourier transform (FFT) and wavelet transform (WT)) [4]-[8]. There are three main techniques for extracting harmonics; (i) frequency domain, (ii) time domain, and (iii) artificial intelligence neural networks techniques.Some drawbacks of using frequency domain techniques are leakage problems, the synchronization between the sampling frequency and the fundamental frequency, the larger memory needed, large number of computations, poor performance during transient, and the filters are not real time. With time domain filters there is a tradeoff between the attenuation and phase delay (higher the attenuation, the lower the phase delay and vice versa), and faster transition time can cause oscillations. The artificial intelligent techniques overcome some of the disadvantages of non-parametric methods. The three main methods used in artificial intelligence techniques are (i) adaptive linear neuron (ADALINE), (ii) the popular back propagation neural networks (BPNN), and (iii) radial function basis neural networks (RBFNN) [9]-[14]. The ADALINE is used as an online harmonics identifier, and its performance depends on the number of harmonics included in its structure. The convergence of the ADALINE slows as the number of harmonics included increases and also subjected to fall in local minima [9]-[12]. The BPNN on the other hand deals with harmonics detection problem as a pattern recognition problem. It uses offline supervised training to identify selected harmonics. The long training time required in BPNN and the chance of falling in local minima is always present [9]-[12]. The RBFNN has several advantages over ADALINE and BPNN; capable of approximating highly nonlinear functions, its structural nature facilitates the training process because the training can be done in a sequential manner, and the use of local approximation can give better generalization capabilities [11, 13,15].

In this paper, RBFNN is used to extract the total harmonics based on p-q theory [6,11, 13,15]. The RBFNN training technique was based on separated and sequential method. The centers of the RBFNN are selected based on K-means clustering method, and the weights of the networks were found based on the direct inversion method.

Instantaneous active and reactive theory (p-q theory) was introduced by H. Akagi, Kawakawa, and Nabae in 1984 [3]. Since then, many scientists and engineers made significant contributions to its modifications in three-phase four-wire circuits and its applications to power electronic equipment. The p-q theory [3] based on a set of instantaneous powers defined in the time domain. No restrictions are imposed on the voltage and current waveforms, and it can be applied to three phase systems with or without neutral wire for three phase generic voltage and current waveforms. Thus, it is valid not only in the steady state, but also in the transient state.

The PI controller [5]-[7] requires precise linear mathematical models, which are difficult to obtain and may not give satisfactory performance under parameter variations, load disturbance etc.The p-q control strategy is unable to yield an adequate solution when source voltages are not ideal. PI controller fails to respond quickly because of the non-linear nature of the system, so we are developing artificial intelligent techniques to analyze the performance of the system under the distorted condition.

2. INSTANTANEOUS ACTIVE AND REACTIVE POWER (p − q) METHOD

The control block diagram for entire p − q scheme is depicted in Figure 1.

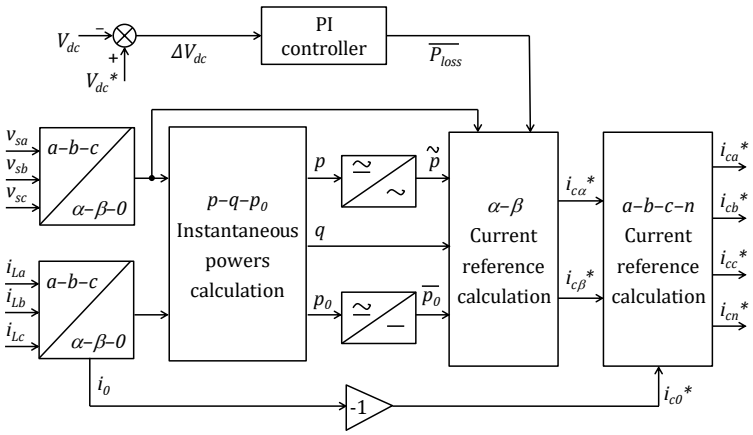

Figure 1. Control block diagram for p − q scheme

The instantaneous load currents in three phases (i_{La}, i_{Lb}, i_{Lc}) and source voltages in three phases (v_{sa}, v_{sb}, v_{sc}) are tracked using sensors, followed by a coordinate transformation from $a-b-c$ to $\alpha-\beta-0$ as follows.

$$\begin{bmatrix} i_0 \\ i_\alpha \\ i_\beta \end{bmatrix} = \sqrt{\frac{2}{3}} \begin{bmatrix} \frac{1}{\sqrt{2}} & \frac{1}{\sqrt{2}} & \frac{1}{\sqrt{2}} \\ 1 & -\frac{1}{2} & -\frac{1}{2} \\ 0 & \frac{\sqrt{3}}{2} & -\frac{\sqrt{3}}{2} \end{bmatrix} \begin{bmatrix} i_{La} \\ i_{Lb} \\ i_{Lc} \end{bmatrix} \quad (1)$$

$$\begin{bmatrix} v_0 \\ v_\alpha \\ v_\beta \end{bmatrix} = \sqrt{\frac{2}{3}} \begin{bmatrix} \frac{1}{\sqrt{2}} & \frac{1}{\sqrt{2}} & \frac{1}{\sqrt{2}} \\ 1 & -\frac{1}{2} & -\frac{1}{2} \\ 0 & \frac{\sqrt{3}}{2} & -\frac{\sqrt{3}}{2} \end{bmatrix} \begin{bmatrix} v_{sa} \\ v_{sb} \\ v_{sc} \end{bmatrix} \quad (2)$$

The instantaneous values of active power (p), reactive power (q) and zero-sequence power (p_0) are calculated by multiplying the instantaneous $\alpha-\beta-0$ components of currents and voltages as per (3). Each of these powers has an oscillating/AC component and an average/DC component as shown in (4), (5) and (6).

$$\begin{bmatrix} p_0 \\ p \\ q \end{bmatrix} = \sqrt{\frac{2}{3}} \begin{bmatrix} v_0 & 0 & 0 \\ 0 & v_\alpha & v_\beta \\ 0 & -v_\beta & v_\alpha \end{bmatrix} \begin{bmatrix} i_0 \\ i_\alpha \\ i_\beta \end{bmatrix} \quad (3)$$

$$p = \bar{p} + \tilde{p} \quad (4)$$

$$q = \bar{q} + \tilde{q} \quad (5)$$

$$p_0 = \overline{p_0} + \widetilde{p_0} \quad (6)$$

Here, $\bar{p}$, $\bar{q}$ and $\overline{p_0}$ are AC components of p, q and p_0 respectively. Similarly, $\tilde{p}$, $\tilde{q}$ and $\widetilde{p_0}$ represent corresponding DC components.For reactive power and harmonic compensation, the entire reactive power (q) and oscillating component of active power $(\tilde{p})$ are utilized for calculation of reference filter currents in $\alpha-\beta$ coordinates using (7).

$$\begin{bmatrix} {i_{c\alpha}}^* \\ {i_{c\beta}}^* \end{bmatrix} = \frac{1}{\sqrt{{v_\alpha}^2 + {v_\beta}^2}} \begin{bmatrix} v_\alpha & -v_\beta \\ v_\beta & v_\alpha \end{bmatrix} \begin{bmatrix} -\tilde{p} + \Delta\bar{p} \\ -q \end{bmatrix} \quad (7)$$

The additional average power required to compensate for the losses occurring inside VSI due to the switching of semiconductor devices is given by (8).

$$\Delta\bar{p} = \overline{p_0} + \overline{P_{loss}} \quad (8)$$

Here, $\overline{p_0}$ is the power required to maintain energy balance inside VSI. Whereas, $\overline{P_{loss}}$ is the average loss occurring inside VSI,which is obtained from DC-link voltage regulator as per (9).

$$\overline{P_{loss}} = K_p \Delta V_{dc} + K_i \int \Delta V_{dc} \cdot dt \quad (9)$$

Finally, reference filter currents in the four wires of VSI can be obtained by following (10) and (11).

$$\begin{bmatrix} i_{ca}^* \\ i_{cb}^* \\ i_{cc}^* \end{bmatrix} = \sqrt{\frac{2}{3}} \begin{bmatrix} \frac{1}{\sqrt{2}} & 1 & 0 \\ \frac{1}{\sqrt{2}} & -\frac{1}{2} & \frac{\sqrt{3}}{2} \\ \frac{1}{\sqrt{2}} & -\frac{1}{2} & -\frac{\sqrt{3}}{2} \end{bmatrix} \begin{bmatrix} i_{c0}^* \\ i_{c\alpha}^* \\ i_{c\beta}^* \end{bmatrix} \quad (10)$$

$$i_{cn}^* = i_{ca}^* + i_{cb}^* + i_{cc}^* \quad (11)$$

3. MODIFIED $p - q$ METHOD

This scheme uses voltage harmonic filtering in order to make the source voltage sinusoidal; before utilizing the same for calculation of instantaneous active and reactive powers. Control block diagram for the entire method of reference current generation using modified p − q scheme is illustrated in Figure 2.

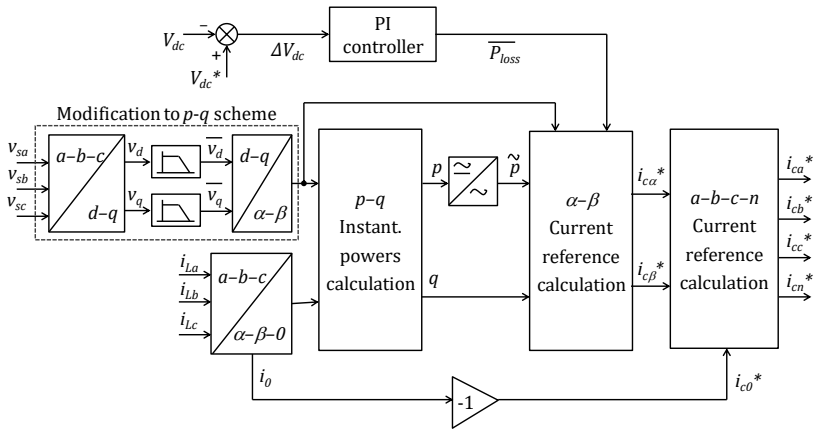

Figure 2. Control block diagram for modified p − q scheme

$$\begin{bmatrix} v_d \\ v_q \end{bmatrix} = \sqrt{\frac{2}{3}} \begin{bmatrix} \sin\omega t & \cos\omega t \\ -\cos\omega t & -\sin\omega t \end{bmatrix} \begin{bmatrix} 1 & -\frac{1}{2} & -\frac{1}{2} \\ 0 & \frac{\sqrt{3}}{2} & -\frac{\sqrt{3}}{2} \end{bmatrix} \begin{bmatrix} v_{sa} \\ v_{sb} \\ v_{sc} \end{bmatrix} \quad (12)$$

$$\begin{bmatrix} v_\alpha \\ v_\beta \end{bmatrix} = \begin{bmatrix} \cos\omega t & \sin\omega t \\ -\sin\omega t & \cos\omega t \end{bmatrix} \begin{bmatrix} \overline{v_d} \\ \overline{v_q} \end{bmatrix} \quad (13)$$

This is followed by the same procedure of reference compensation current extraction as done in case of conventional p − q method.

4. RADIAL BASIS FUNCTION NETWORK

4.1. Structure of RBFNN

RBF is a new method of designing a neural network as a curve fitting problem in a high dimensional space. According to this, learning is equivalent to find a surface in a multidimensional space that provides a best fit to the training data. The motivation behind RBF is to interpolate the test data in a multidimensional space.In a neural network the hidden units provides a set of functions that constitute an arbitrary 'basis' for the input pattern when they are expanded into the hidden space. These functions are called Radial basis function (RBF).

The construction of RBF involves three layers with entirely different role, one input layer source nodes with inputs I1, I2 , … , IN), one hidden layer has K neurons, and one output layer (with outputs y1, y2, …, ym). The input-output mapping consists of two different transformations; nonlinear transformation from

the input layer to the hidden layer and linear transformation between hidden and output layers. The connection between the input and hidden layers is called centers and the connection between the hidden and output layers is called weights.The overall response of the RBF network is

$$f_{xy} = \sum_{i=1}^{n} w_i \, \emptyset(\|y - c_i\|^2/\rho_i) \quad (14)$$

where 'n' is the number of computing units 'c' is the RBF center,ρ is the width of the units and 'w' is the weight. All widths have same value. The basis functions are usually selected as Gaussian. Although other choices could be made for the basis function Gaussians are almost always used as they enjoy several desirable properties from point of view of interpolation and regularization theory.

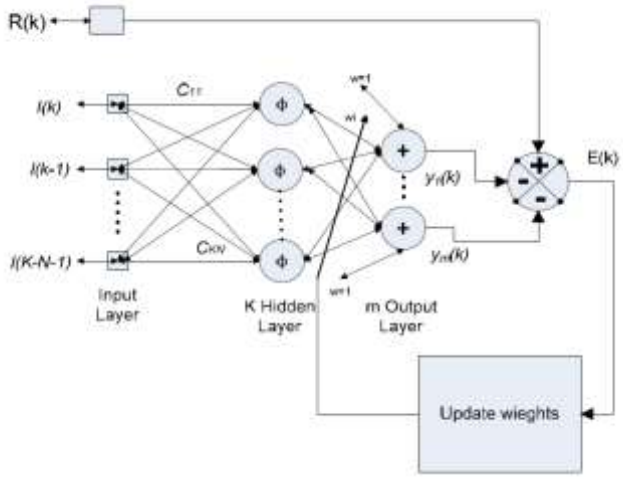

Figure 3. Basic structure for an adaptive RBF network

For RBF network determining the number and location of center is a difficult part of design. Clustering techniques are commonly used to reduce the number of centers to a single point. Whether the RBF network can realize optimal solution depends crucially on whether the centers can be positioned correctly or not.During the training period the position of each RBF center is defined by the transmission of known data sequence. The center position can be approximated as closely as desired by clustering or averaging the centers found during several repetitions.

4.2. Learning Algorithm

The unit centers should be placed in those regions of the input space where data is present. Unfortunately, this means that as the input vector dimension grows the number of required units' increases very rapidly. Another reason for using a large number of local units before linear combination is given by Cover's separatebility theorem, which states that in general, a complex pattern classification problem cast in high dimensional space none linearly is more likely to be linearly separable then in low dimensional space. This increase in the number of units is the price to be paid for a structure whose weight can be trained much faster than in conventional the multilayer neural network.

The RBF learning algorithm is usually decoupled in two steps. First clustering is performed on the input vectors to determine the unit centers and radij and then output weights are adjusted [11, 13, 15]. The first step is accomplished using an unsupervised clustering algorithm and radij are chosen with k-nearest neighbor heuristic. Then keeping the center and radij fixed the weights are computed in closed form using desired output. The weights matrix w is given by

$$W=A^{-1}\emptyset^{T}D \quad (15)$$

Where D is the desired output vector for l training data samples set. The summation of the outputs of the RBFNN model is equal to the reference signal R(k). In this case the error E(k) equal to zero and no change in the RBFNN weight

$$E(k) = R(k) - \{y_1(k) + y_2(k) + \cdots + y_m(k)\} \quad (16)$$

The error E(k) is used to update the weights vectors based on the least-mean- square-error algorithm.

$$w_{1new} = w_{1old} + \eta_1 \phi(k) E(k) \quad (17)$$

$$w_{mnew} = w_{mold} + \eta_m \phi(k) E(k) \quad (18)$$

where ηj is the regulation factor for the jth output node.The weights updating will continue until the error E(k) become zero again.

5. METHODOLOGY

5.1. RBFN For p-q Theory

The three phase source voltages and load currents are sampled and used to calculate the instantaneous active power p and imaginary power q based on p-q theory. Clark transformation is used to transform the voltages and currents from a-b-c domain to α-β domain as shown in (1) and (2). The p and q are calculated from α-β domain voltages and currents as shown in (3). The reference current in α-β domain can be calculated as shown in (7) and then the reference current in a-b-c domain can be calculated as shown in (11).

5.2. Building the Delay Buffer

Instantaneous active power Sampled at constant rate and passed through the first input first output (FIFO) buffer to create a delayed vector with length N which match the length of the input vector of RBFNN. At any instant the FIFO buffer will contain N data samples. The training data samples for l training data samples is written in matrix form and given by

$$X = \left| x_1 \quad x_2 \ldots . x_l \right| = \begin{vmatrix} p_{11} & p_{12} & \ldots . & p_{1l} \\ p_{21} & p_{22} & \ldots . & p_{2l} \\ . & . & \ldots . & \\ . & . & \ldots . & \\ p_{N1} & p_{N2} & \ldots . & p_{Nl} \end{vmatrix} \quad (19)$$

5.3. Finding the Desired Output

For each x_j fast Fourier transform (FFT) is used to find the constant (DC) part of the active power (which represents the power due to the fundamental components). The constant part obtained from applying the FFT on *x'*s data become the desired output mentioned in [10] and given as equation (20). since the number of the output nodes is one only the DC component of FFT is taken which is a scalar quantity.

$$\text{FFT}\{x_j\} = d_i^{DC} \quad (20)$$

5.4. Training Data Generation

For the Extraction of sequence currents, the inputs are the three phase current and the corresponding outputs. The required inputs and outputs are generated in MATLAB program. In the program the input currents are initialized to zero, and incremented in steps. By taking one thousand samples in a cycle and arranging them in a vector of three rows, outputs arranged in required vector size depends on the number of the outputs. The input vector size and output vector size must have the same number of columns. The training data is generated for ideal and distorted conditions.

The training of the network was done with MATLAB program. First clustering was performed on the input vectors to determine the unit centers and radii and then output weights are adjusted. This was accomplished using unsupervised clustering algorithm and radij are chosen with K-nearest neighbor heuristic. Then, keeping the center and radij fixed the weights are computed in closed form using the desired output. The training was done for both ideal and distorted source voltage conditions. After training the network was simulated with trained inputs, If the network errors are within the predefined range, then the architecture is suitable, otherwise the network architecture must be changed. After training the architecture is converted to simulink block.

6. SIMULATION RESULTS AND DISCUSSION

Extensive investigations are carried out by performing simulations in order to find out the effectiveness of the three discussed APF control schemes. System configuration of shunt APF along with three-phase and single-phase nonlinear diode rectifier loads is depicted in Figure 4.

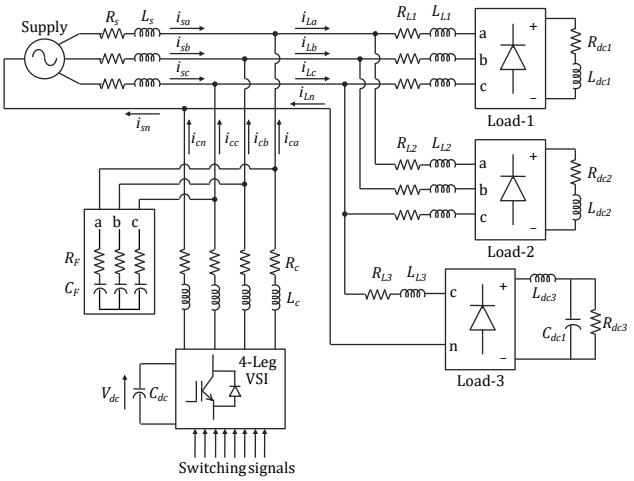

Figure 4. Three-phase four-wire APF system configuration with nonlinear loads

The values of system parameters used for simulation are indicated in Table 1. Demonstration is done under two different conditions of supply voltage. For ideal supply, completely balanced and sinusoidal voltage of 230 V RMS is considered. Distorted supply condition is created by incorporating 3rd harmonic component into the supply voltage.

Table 1. Values of system parameters used in simulation

Parameter	Notation	Value
Supply frequency	f	50 Hz
Source impedance	(R_s, L_s)	$(10\ \text{m}\Omega, 50\ \mu\text{H})$
Load-1 parameters	(R_{L1}, L_{L1}),(R_{dc1}, L_{dc1})	$(0.1\ \Omega, 3\ \text{mH})$, $(25\ \Omega, 25\ \text{mH})$
Load-2 parameters	(R_{L2}, L_{L2}),(R_{dc2}, L_{dc2})	$(0.1\ \Omega, 3\ \text{mH})$, $(25\ \Omega, 60\ \text{mH})$
Load-3 parameters	(R_{L3}, L_{L3}), $(R_{dc3}, L_{dc3}, C_{dc1})$	$(1.5\ \Omega, 15\ \text{mH})$, $(25\ \Omega, 50\ \text{mH}, 540\ \mu\text{F})$
DC-link capacitance	C_{dc}	3 mF
Reference DC-link voltage	$V_{dc}{}^{*}$	800 V
AC-side filter parameters	(R_c, L_c),(R_F, C_F)	$(0.1\ \Omega, 1\ \text{mH})$, $(0.5\ \Omega, 25\ \mu\text{F})$

Initially, only Load-1 is put into operation until $t = 0.1$ s,to evaluate the harmonic compensation capability. Performance under dynamic conditions is observed by sudden switching on of Load-2 and 3 at $t = 0.1$ s for compensation of current harmonics, neutral current and unbalanced source current resulted due to the single-phase load (Load-3).

Simulation results for APF employing $p - q$, modified $p - q$ and RBFNN-PQ control schemes under ideal supply voltage condition are shown in Figures 5. The supply voltage (V_s), load current (i_L), compensation currents in phases a, b and c(i_{ca}, i_{cb}, i_{cc}), neutral current (i_n) and source current (i_s) waveforms are presented in top to bottom order. The nature of source current before compensation is exactly same as the load current. Neutral current, that is the current flowing in neutral conductor comes into significance only during the time unbalance in load current exists, that is from $t = 0.1$ sto $t = 0.2$ s. The current harmonics, neutral current and unbalance have been successfully cancelled with all the three control methods.

Simulation results for APF employing $p - q$, modified $p - q$ and RBFNN-PQ control schemes under distorted supply voltage condition are shown in Figure 6. It depicts the supply voltage (V_s), load current (i_L), compensation currents in phases a, b and c(i_{ca}, i_{cb}, i_{cc}), neutral current (i_n) and source current

(i_s) waveforms in top to bottom order. Current harmonics, neutral current and unbalance in source current have been compensated employing all the discussed control schemes.

FFT analysis is performed in order to figure out the overall THD in the three phases of source current under all the two supply conditions, before and after compensation with the three control schemes. The source current THDs without and with APF employing $p-q$, modified$p-q$ and RBFNN-PQ control schemes under ideal and distorted supply conditions are clearly presented in Table.2 and Table.3 respectively.

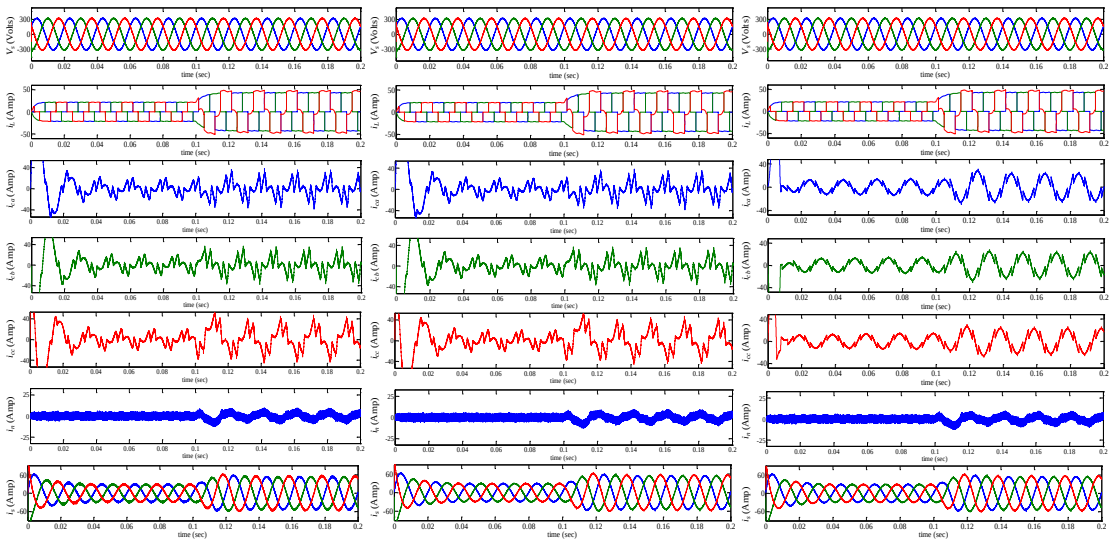

(a) (b) (c)

Figure 5. Ideal supply. Supply voltage (V_s), load current (i_L), compensation currents in phases a, b and c(i_{ca}, i_{cb}, i_{cc}), neutral current (i_n) and source current (i_s) waveforms under ideal supply condition for APF employing: (a) $p-q$ control scheme (b) modified $p-q$ control scheme (c) RBFNN-PQ control scheme

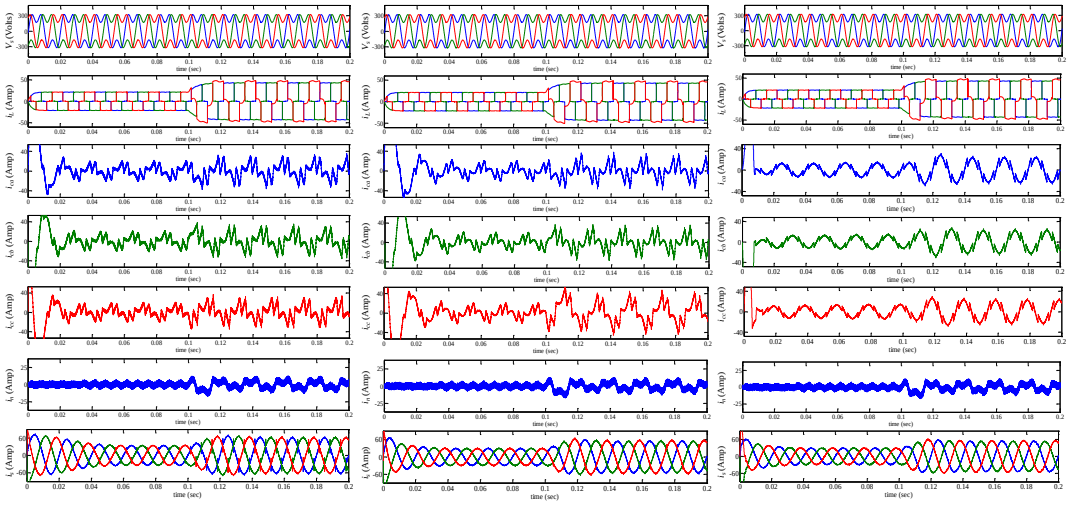

(a) (b) (c)

Figure 6. Distorted supply. Supply voltage (V_s), load current (i_L), compensation currents in phases a, b and c(i_{ca}, i_{cb}, i_{cc}), neutral current (i_n) and source current (i_s) waveforms under distorted supply condition for APF employing: (a) $p-q$ control scheme (b) modified $p-q$ control scheme (c) RBFNN-PQ control scheme

Table 2. Chart diagram showing source current THDs (in %) before and after compensation with p − q, modifiedp − q and RBFNN-PQ control schemes for simulations under ideal supply condition

	Phase-a	Phase-b	Phase-c
Without APF	30.13	30.05	28.38
p-q Scheme	4.12	4.03	3.72
Modified p-q Scheme	3.41	3.46	3.14
RBFNN-PQ	3.07	3.03	2.94

Table 3. Chart diagram showing source current THDs (in %) before and after compensation with p − q, modifiedp − q and RBFNN-PQ control schemes for simulations under distorted supply condition.

	Phase-a	Phase-b	Phase-c
Without APF	30.78	30.77	28.23
p-q Scheme	6.78	6.56	6.17
Modified p-q Scheme	4.39	4.31	4.05
RBFNN-PQ	3.62	3.54	3.68

It is clearly observed from the simulation results obtained under ideal supply that, the THD in source current has been lowered down to nearly 3% with p − q and modified p − q schemes from the uncompensated source current THD of nearly 30%. However, RBFNN-PQ scheme is found to be more proficient, as it lowers down the source current THD to nearly 3.5% even during large change in load and unbalanced loading conditions. Hence, all the control schemes are found to be successful in lowering down the THDs in source current well below 5%. Under highly distorted supply, though modified p − q scheme works comparatively better than p − q scheme, RBFNN-PQ scheme outperforms the other two schemes by lowering down the source current THDs in three phases to 3.62%, 3.54% and 3.68% even under sudden load change and unbalanced loading conditions.

7. CONCLUSION

A comparison between the Conventional p-q, modified p-q and RBFNN-PQ control schemes for three-phase four-wire VSI-based APF is realized. The reference compensation currents for the four-wires are extracted and Hysteresis PWM is carried out to generate switching signals for VSI. DC-link voltage has been regulated successfully using a PSO-based PI controller, minimizing the undesirable power loss responsible for degradation of APF performance, thereby providing optimal load compensation. MATLAB/Simulink results showing the response of the control schemes under transient and steady-state conditions are presented. All the control schemes discussed here are effective in harmonic compensation under ideal supply and satisfy the IEEE-519 Standards on harmonic limits. Under distorted supply, though modified p-q scheme lowers down the THD to values smaller than Conventional p-q, it fails to bring down the THD below 5%, which can be seen from Table 3. In contrast, RBFNN-PQ scheme yields the lowest values of source current THDs. The excessive neutral current has been compensated by all the control schemes under all kinds of supplies. This proves that, RBFNN-PQ scheme is the best control scheme to be employed in shunt APF compared to the other two mentioned control schemes.

REFERENCES

[1] H. Akagi, "New trends in active filters for power conditioning," *Industry Applications, IEEE Transactions on, vol. 3*2, pp. 1312-1322, 1996.
[2] T. C. Green and J. H. Marks, "Control techniques for active power filters," *Electric Power Applications, IEE Proceedings*, vol. 152, pp. 369-381, 2005.
[3] H. Akagi, H. Kanazawa and Y. Nabae, "Instantaneous Reactive Power Compensators Comprising Switching Devices without Energy Storage Components*," IEEE Transactions on Industry Applications*, vol. IA-20, no. 3, pp. 625-630, 1984.
[4] Z. Peng, et al., "Harmonic and Reactive Power Compensation Based on the Generalized Instantaneous Reactive Power Theory for Three-Phase Four-Wire Systems," *IEEE Transactions on Power Electronics*, vol. 13, no. 5, pp. 1174-1181, 1998.
[5] B. Singh, K. Al-Haddad and A. Chandra, "A review of active filters for power quality improvement," *Industrial Electronics, IEEE Transactions on*, vol. 46, pp. 960-971, 1999.
[6] S. Mikkili and A. K. Panda, "Simulation and RTDS Hardware Implementation of SHAF for Mitigation of Current Harmonics with p-q and id-iq Control Strategies Using PI Controller," *International Journal of Engineering, Technology & Applied Science Research*, vol. 1, no.3, 2011, pp. 54-62.

[7] M. Suresh, A. K. Panda and Y. Suresh, "Fuzzy Controller Based 3-Phase 4-Wire Shunt Active Filter for Mitigation of Current Harmonics with Combined p-q and id-iq Control Strategies," Journal of Energy and Power Engineering, Vol. 3, No. 1, 2011, pp. 43-52.
[8] Y.Kusuma Latha, Ch.Saibabu, Y.P.Obulesh" Control Strategy for Three Phase Shunt Active Power Filter with Minimum Current Measurements," *International Journal of Electrical and Computer Engineering (IJECE)*, vol.1, no.1, pp. 31-42, 2011.
[9] S. S. Haykin 1931-, Neural Networks: A Comprehensive Foundation /. Upper Saddle River, N.J.: Prentice Hall, c1999.
[10] J.Moody, "Fast learning in networks of locally-tuned processing units", *Neural Computing*, vol.1, pp.281, 1989.
[11] G. W. Chang, Cheng-I Chen and Yu-Feng Teng, "Radial-Basis-Function-Based Neural Network for Harmonic Detection, " *IEEE Transactions on Industrial Electronics*, vol. 57, pp. 2171-2179, 2010.
[12] A. Zouidi, F. Fnaiech, K. Al-Haddad and S. Rahmani, "Adaptive linear combiners a robust neural network technique for on line harmonic tracking," *Industrial Electronics, 2008. IECON 2008. 34th Annual Conference of IEEE*, pp. 530-534, 2008.
[13] R. Yousef, "Training radial basis function networks using reduced sets as center points," *International Journal of Information Technology*, vol. 2, pp. 21, 2005.
[14] Mridul Jha, S.P. Dubey ," Neuro-Fuzzy based Controller for a Three-Phase Four-Wire Shunt Active Power Filter", *International Journal of Power Electronics and Drive System (IJPEDS)*, vol.1, no.2, pp. 148~155, 2011.
[15] G. W. Chang, C. I. Chen, Y. F. Teng " An Application of Radial Basis Function Neural Network For Harmonics Detection," *in Proc 2008 Harmonics and Quality of Power 13th International Conference*, pp.1-5.

BIOGRAPHIES OF AUTHORS

Prakash Chandra Tah received his Bachelors in Electrical Engineering from Indira Gandhi Institute of Technology,Odisha, India in 2002. He completed his Masters in Technology (Electronics system and communication) from National Institute of Technology Rourkela, Rourkela, India in 2005.He worked asSr. Lecturer and Assistant Professor for four year in the Electrical and Electronics Engineering Dept. of KIIT University. Currently he is working as a Sr.Tech.in Power and blowing station,Rourkela steel plant,SAIL. His current research interests include power converters, active filtering, power conditioning, AC and DC drives, neural network and fuzzy logic based controller design for Electrical drives, Genetic Algorithm Optimization.

Anup Kumar Panda:. He received the B.Tech in Electrical Engineering from Sambalpur University, India in 1987. He received the M.Tech in Power Electronics and Drives from Indian Institute of Technology, Kharagpur, India in 1993 and Ph.D. in 2001 from Utkal University. Join as a faculty in IGIT, Sarang in 1990. Served there for eleven years and then join National Institute of Technology, Rourkela in January 2001 as an assistant professor and currently continuing as a Professor in the Department of Electrical Engineering. He has published over hundred articles in journals and conferences. He has completed two MHRD projects and one NaMPET project. Guided eight Ph.D. scholars and currently guiding twelve scholars in the area of Power Electronics & Drives. His research interest includes Design of high frequency power conversion circuits and Applications of Soft Computing Techniques, improvement in Multilevel Converter Topology, Power Factor Improvement, Power quality Improvement in power system and Electric drives.

Bibhu Prasad Panigrahi: He received the B.Sc.(Engineering) degree in Electrical Engineering with Honors from VSSUT, Burla (then University College of Engineering, Burla, Sambalpur University) Odisha, India in the year 1989 and the M.Tech. (Power Electronics and Power Systems) degree from Indian Institute of Technology, Bombay, Mumbai, India in the year 1997. He obtained his Ph.D. degree in Electrical Engineering from Indian Institute of Technology, Kharagpur, India in the year 2007. He has worked as Assistant Engineer in Fertilizer Corporation of India Limited for two years from 1989 to 1991. After spending few months as Executive Trainee in Nuclear Power Corporation of India Limited, he switched over to academics and joined Electrical Engineering Department of Indira Gandhi Institute of Technology (IGIT), Sarang, Dhenkanal, Orissa (India) as a Lecturer in April 1992. In April 1997, he became Senior Lecturer in the same department and in April 2002, he was promoted to Lecturer (Selection Grade)/Assistant Professor. In March 2009, he joined as Professor in the same Electrical Engineering Department of IGIT, Sarang and heading the department since then. He has published forty nine research papers in various journals and conference proceedings both at national and international level. His research interest includes Electrical Machines, Power Electronics and Power System.